Environmental Science & Technology

Article

pubs.acs.org/est

Estimates of Health Impacts and Radiative Forcing in Winter Haze in Eastern China through Constraints of Surface $PM_{2.5}$ Predictions

Meng Gao,[*,†,‡] Pablo E. Saide,[§] Jinyuan Xin,[∥] Yuesi Wang,[∥] Zirui Liu,[∥] Yuxuan Wang,[⊥,#] Zifa Wang,[∥] Mariusz Pagowski,[▽] Sarath K. Guttikunda,[○] and Gregory R. Carmichael[*,†,‡]

[†]Department of Chemical and Biochemical Engineering, University of Iowa, Iowa City, Iowa 52242, United States

[‡]Center for Global and Regional Environmental Research, University of Iowa, Iowa City, Iowa 52242, United States

[§]Atmospheric Chemistry Observations and Modeling (ACOM) Lab, National Center for Atmospheric Research (NCAR), Boulder, Colorado 80305, United States

[∥]State Key Laboratory of Atmospheric Boundary Layer Physics and Atmospheric Chemistry, Institute of Atmospheric Physics, Chinese Academy of Sciences, Beijing, China

[⊥]Department of Earth and Atmospheric Sciences, The University of Houston, Houston, Texas 77004, United States

[#]Ministry of Education Key Laboratory for Earth System Modeling, Center for Earth System Science, Tsinghua University, Beijing, China

[▽]NOAA Earth System Research Laboratory (ESRL), Boulder, Colorado 80305, United States

[○]Division of Atmospheric Sciences, Desert Research Institute, Reno, Nevada 89119, United States

Supporting Information

ABSTRACT: The Gridpoint Statistical Interpolation (GSI) Three-Dimensional Variational (3DVAR) data assimilation system is extended to treat the MOSAIC aerosol model in WRF-Chem, and to be capable of assimilating surface $PM_{2.5}$ concentrations. The coupled GSI-WRF-Chem system is applied to reproduce aerosol levels over China during an extremely polluted winter month, January 2013. After assimilating surface $PM_{2.5}$ concentrations, the correlation coefficients between observations and model results averaged over the assimilated sites are improved from 0.67 to 0.94. At nonassimilated sites, improvements (higher correlation coefficients and lower mean bias errors (MBE) and root-mean-square errors (RMSE)) are also found in $PM_{2.5}$, PM_{10}, and AOD predictions. Using the constrained aerosol fields, we estimate that the $PM_{2.5}$ concentrations in January 2013 might have caused 7550 premature deaths in Jing-Jin-Ji areas, which are 2% higher than the estimates using unconstrained aerosol fields. We also estimate that the daytime monthly mean anthropogenic aerosol radiative forcing (ARF) to be $-29.9 W/m^2$ at the surface, $27.0 W/m^2$ inside the atmosphere, and $-2.9 W/m^2$ at the top of the atmosphere. Our estimates update the previously reported overestimations along Yangtze River region and underestimations in North China. This GSI-WRF-Chem system would also be potentially useful for air quality forecasting in China.

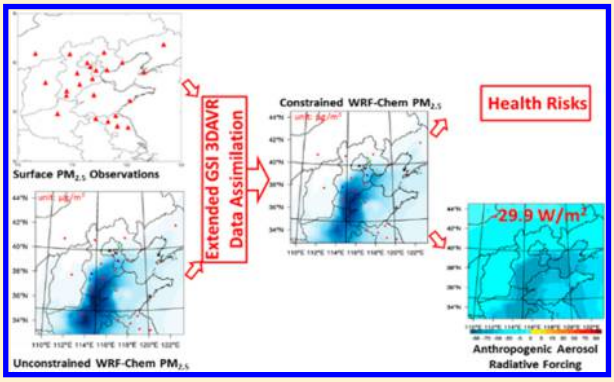

INTRODUCTION

As the most populous developing country in the world, China is facing serious air pollution. Fine particulate matter ($PM_{2.5}$) levels in China are among the highest in the world.[1] According to the assessment of burden of disease, ambient PM pollution is the fourth highest risk in East Asia (China), leading to 1.2 million deaths in China in 2010.[2] Frequent winter haze events have been happening over the North China Plain[3−5] with estimated significant short-term health consequences.[6] Thus, providing reliable $PM_{2.5}$ predictions is particularly important for the public to avoid health consequences, and for the policy makers to help design effective control measures. High PM levels also directly interact with radiation, and modify cloud properties to affect the Earth's radiation budget[7] as well as dynamics of the atmosphere;[8] and interactions may lead to even higher near surface concentrations (through reductions in mixing layer heights and wind speeds).[3,4] Although there have been great advances in predicting aerosols, it is still challenging to predict PM levels during haze events due to imperfect model parametrization, incomplete understanding of aerosol formation and large uncertainties in emission inventories.[3,9]

Received: July 26, 2016
Revised: January 12, 2017
Accepted: January 19, 2017
Published: January 19, 2017

DOI: 10.1021/acs.est.6b03745
Environ. Sci. Technol. 2017, 51, 2178−2185

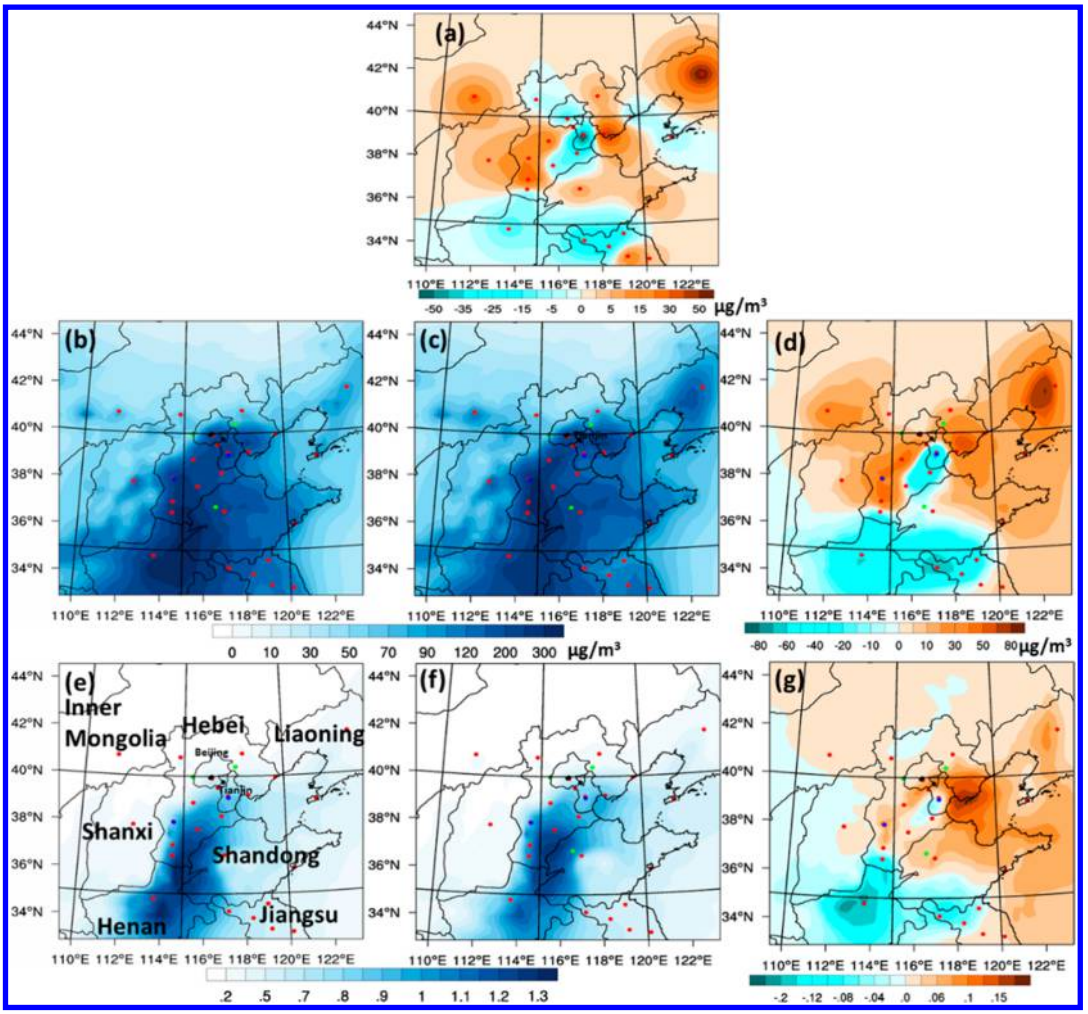

Figure 1. Monthly average analysis increments (a), mean surface $PM_{2.5}$ and AOD at 600 nm in NODA case (b,e), DA case (c,f) and the differences (DA minus NODA) (d,g); CNEMC sites are in red.

Computation of the estimated health impacts of aerosols and estimates of the radiative forcing caused by these aerosols require the use of both better models and more/all available observational data. Data assimilation (DA) is a powerful technique to combine model results and observations to reduce uncertainties in predicted distributions.[10,11] DA has been widely used in meteorology for more than three decades, but its application in air quality modeling is relatively recent,[12,13] and efforts have been hampered by the lack of key measurements and their availability in near real time. With the progress in establishing multiple chemical measurement platforms, the chemical DA area is growing fast. Chemical DA was initially applied to integrate trace gases.[14−19] Later, aerosol measurements including Aerosol Optical Depth (AOD) from multiple platforms (such as CALIOP, MISR, MODIS) have been assimilated using various methods, including optimal interpolation,[13,20,21] 3DVAR,[10,11,22−29] 4DVAR,[30] and EnKF.[12,31−34] Aerosol DA has also been applied in operational aerosol forecasting.[30,35] Most of the past work on chemical DA has been done using offline models; less research has been performed using online coupled models.[36] A more thorough review of DA for atmospheric chemistry can be found in Bocquet et al. (2015).[36] The use of AOD observations is limited during heavy haze events as the retrievals are mostly missing when severe haze occurs over China. Since January 2013, China National Environmental Monitoring Center (CNEMC) released the real-time observations of $PM_{2.5}$ and PM_{10}. This data set along with the improvements of computational resources will facilitate further studies of aerosol DA in China.

In this study, we incorporate surface $PM_{2.5}$ and evaluate its impact in better constraining surface $PM_{2.5}$ levels during heavy haze. Although ground-based and satellite observations have been assimilated over China,[24,25] to our knowledge this is the first attempt to apply DA technique to overcome difficulties in modeling winter haze event in North China. The improvements in surface $PM_{2.5}$ predictions by applying DA to integrate $PM_{2.5}$ measurements are validated using independent observations of surface PM and AOD. The impacts of DA on estimates of health impacts and radiative forcing are also evaluated.

MATERIALS AND METHODS

WRF-Chem Model Configurations. WRF-Chem is used to simultaneously simulate meteorology and chemistry and the effects of aerosols on radiation and cloud formation. We have used this model to simulate winter haze evolution,[3−5] evaluate health and economic losses,[6] and provide operational air quality forecast in China. In this study, the model is configured with two nested domains with 80 × 56 (81km resolution) and 48 × 48 (27 km resolution) grids (as shown in Figure S1 in Supporting Information (SI)). Initial and boundary conditions

DOI: 10.1021/acs.est.6b03745
Environ. Sci. Technol. 2017, 51, 2178−2185

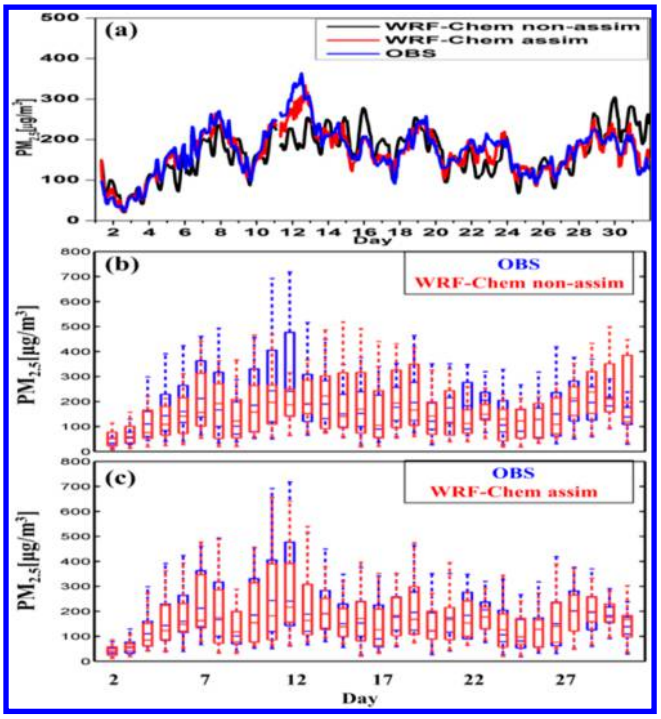

Figure 2. Observed and simulated (DA and NODA) hourly $PM_{2.5}$ concentrations averaged over CNEMC measurement sites (a), and whisker plots for observed daily mean $PM_{2.5}$ concentration and simulations in NODA case (b) and DA case (c).

Table 1. Statistics[a] for Simulated $PM_{2.5}$ With and Without DA Compared Against CNEMC Observations

	MBE ($\mu g/m^3$)	MAE ($\mu g/m^3$)	MFB	MFE	RMSE ($\mu g/m^3$)	R
NODA	−6.1	37.0	−3.0%	20%	38.0	0.67
DA	−3.8	14.9	−1.0%	10%	20.5	0.94

[a]MBE = mean bias error; MAE = mean absolute error; MFB = mean fractional bias; MFE = mean fractional error; RMSE = root-mean-square error.

for chemicals are taken from global MOZART forecasts.[37] Meteorological initial and boundary conditions are from the ECMWF operational forecasts. We use the Carbon-Bond Mechanism Z (CBMZ) to simulate gas phase chemistry[38] and the Model for Simulating Aerosol Interactions and Chemistry (MOSAIC)[39] to simulate aerosol evolution. Longwave and shortwave radiation are both treated using the RRTMG radiation scheme.[40] Planetary boundary layer evolution is simulated using the Yonsei University parametrization.[41] The Lin parametrization[42] for microphysics and Grell-3D cumulus parametrization[43] are used to simulate aerosol-cloud interactions and precipitation.

The anthropogenic emissions are obtained from the MIX inventory[44] for year 2010. This inventory was made monthly and the spatial resolution is 0.25° × 0.25°.[44] The emission maps of selected gaseous and aerosol species are shown in Figure S2 in SI. Terrestrial biogenic emissions are estimated using the MEGAN[45] model. Windblown GOCART dust[46] emissions and parametrized sea salt emissions are also included and calculated online in the model.

GSI 3DVAR DA System. The GSI 3DVAR DA system provides an analysis by minimizing the cost function as shown below:

$$J(\mathbf{x}) = (x - \mathbf{x}_b)^T \mathbf{B}^{-1}(\mathbf{x} - \mathbf{x}_b) + (\mathbf{y} - H(\mathbf{x}))^T \mathbf{R}^{-1}(\mathbf{y} - H(\mathbf{x}))$$

In this equation, $\mathbf{x}$ is the analysis vector, $\mathbf{x}_b$ denotes the forecast or background vector, $\mathbf{y}$ is an observation vector, $\mathbf{B}$ represents the background error covariance matrix, and $\mathbf{R}$ represents the observation error covariance matrix. H is the observation operator to transform model grid point values to observed quantities which is done by interpolating. In this study, the total mass in each size bin instead of each $PM_{2.5}$ component, is used as control variable, which efficiently reduces the computational complexity.[24] The changes within GSI are distributed considering the mass contribution of each $PM_{2.5}$ component as a constant for each size bin.[24] The standard deviations and vertical as well as horizontal length scales used for computing the background error covariance statistics (BECs) are calculated using the NMC method (Figure S3 in SI).[47] This method commonly uses 24- and 48 h forecasts or 12- and 24 h forecasts to compute statistics, but since we perform retrospective simulations, we use two simulations forced by different meteorology (NCEP FNL analysis and ECMWF reanalysis) to calculate the error statistics.[48] How NMC method calculates standard deviations and length scales (horizontal and vertical) are documented in reference.[49]

Hourly surface $PM_{2.5}$ concentrations from the CNEMC network within 1 h window of the analysis were assimilated. The observation errors contain two parts: measurement errors and representativeness errors. The measurement error was computed using $\varepsilon_o = 1.5 + 0.0075 \times \mathrm{Obs}$[11,24] where Obs means observation values. The representativeness errors depend on the locations of the measurement sites and model resolution, which were calculated as $\varepsilon_r = \gamma\varepsilon_o\sqrt{\frac{\Delta x}{L}}$.[11,24,49] In this calculation, γ is the adjustable scale factor (we used 0.5 following Schwartz et al. (2012)[11]), Δx is model grid resolution, and L is the influencing radius. The used L values vary among different station types: 2000 for urban sites and 10 000 for rural sites, following previous applications in the U.S.[11] and China.[24]

Observational Data. CNEMC has released hourly concentrations of CO, O_3, SO_2, NO_2, $PM_{2.5}$, and PM_{10} in 74 major cities since January 2013. These data can be accessed via http://113.108.142.147:20035/emcpublish/. The data used in this study is the averaged $PM_{2.5}$ concentration in each city (the number of stations in each city ranges from 4 to 13), which represents the average pollution level for each city. The use of averaged data over a city is consistent with the grid-cell resolution used in the inner domain of the model (i.e., 27 km). Air quality data during this study period was also collected by the CARE-China[50] and the CSHNET[51] networks. Hourly $PM_{2.5}$ and PM_{10} concentrations from four observation sites (Beijing, Tianjin, Shijiazhuang, Xianghe) from the CARE-China[50] network are used to evaluate the impacts of assimilating CNEMC $PM_{2.5}$ data. AOD data at three CSHNET[51] sites and at three AERONET[52] sites are also used in this study (locations are shown in Figure S1 in SI).

EXPERIMENTAL DESIGN

Three model runs (DA, NODA/CTL, and ARF0) were done for the period 1 to 31 January 2013. Assimilation of data occurred at 00:00, 03:00, 06:00, 09:00, 12:00, 15:00, 18:00, and 21:00 UTC. ANT0 was conducted without including anthropogenic emissions.

DOI: 10.1021/acs.est.6b03745
Environ. Sci. Technol. 2017, 51, 2178−2185

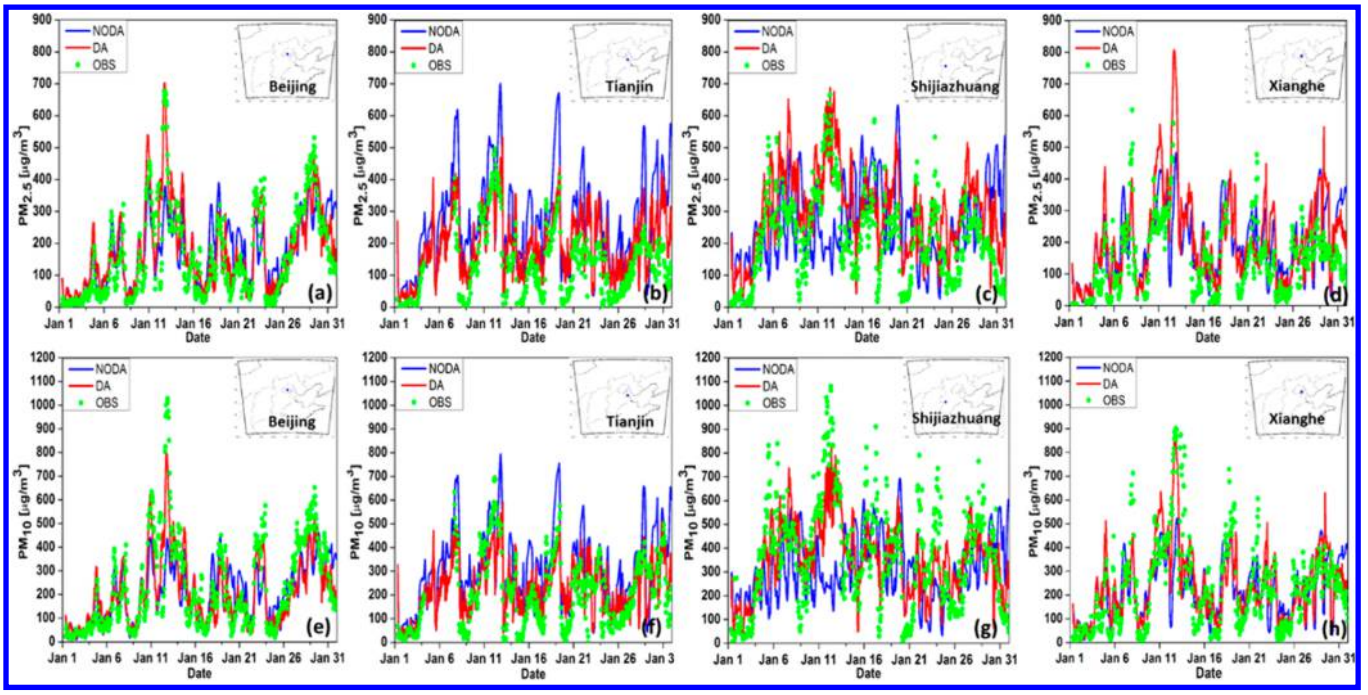

Figure 3. Comparisons between simulated and observed hourly $PM_{2.5}$ (a-d) and PM_{10} (e–h) concentrations at four nonassimilated sites from CARE-China network: Beijing (a, e), Tianjin (b, f), Shijiazhuang (c, g) and Xianghe (d, h).

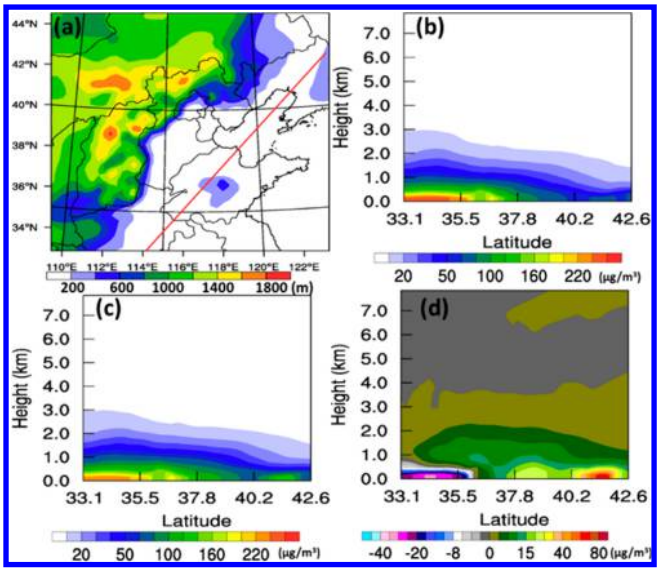

Figure 4. Terrain heights and direction of cross section plots (a); cross section plots of monthly mean $PM_{2.5}$ concentrations in NODA case (b), DA case (c), and the differences (DA-NODA) (d).

RESULTS AND DISCUSSION

Impact of Assimilation on PM and AOD. Figure 1(a) shows the average analysis increments for DA experiment. DA generally increases $PM_{2.5}$ in south and north Hebei, Liaoning, Shanxi and Inner Mongolia, and decreases $PM_{2.5}$ in Tianjin, Henan and west Shandong. The differences between monthly mean $PM_{2.5}$ in the DA and NODA cases exhibit similar spatial distributions (Figure 1(c)), with maximum positive changes (more than 80 $\mu g/m^3$) in Liaoning and maximum negative changes in northwest Jiangsu area. The assimilated $PM_{2.5}$ surface concentrations much better represent the actual distributions of $PM_{2.5}$. Figure 2(a) shows observed and predicted surface $PM_{2.5}$ hourly concentrations averaged over all CNEMC measurement sites. The calculated performance metrics are listed in Table 1. In general, the model captures the aerosol variations of this event. However, $PM_{2.5}$ concentrations are largely underestimated during the 12–14 January haze episode (NODA case), which is likely due to the difficulty of the model in capturing the extreme stable conditions during this time period and a slow sulfate production rate.[3,5,53] The NODA case also overestimates $PM_{2.5}$ in the last several days of January. The monthly averaged MBE is −6.1 $\mu g/m^3$ for the NODA case (Table 1). These underestimations and overestimations are corrected by assimilating surface $PM_{2.5}$. The correlation coefficient between predicted and observed $PM_{2.5}$ averaged over all CNEMC stations increases from 0.67 to 0.94 (Table 1) when DA is used. MBE decreases to −3.8 $\mu g/m^3$, RMSE decreases from 38.0 $\mu g/m^3$ to 20.5 $\mu g/m^3$, and MFE decreases from 22% to 10% (Table 1).

Further details regarding the improvements when using DA is shown in the whisker plots of observed daily mean $PM_{2.5}$ concentrations and predictions for NODA and DA cases (Figure 2(b,c)). The minimum (across all CNEMC sites) daily mean $PM_{2.5}$ concentrations are captured well, but large discrepancies exist in maximum values and median values, particularly during the 12–14 January haze episode. After DA, these discrepancies have been significantly reduced (Two-sample t tests were conducted for maximum and median values from model and observations. After DA, two-sample t tests show that there are no significant differences between modeled and observed maximum and median values at the 5% significance level); median and maximum values of forecasts in DA case all show excellent agreement with observations. The variability in the assimilation distributions also closely matches that in the observations.

The performance of $PM_{2.5}$ assimilation was also evaluated using hourly surface $PM_{2.5}$ and PM_{10} concentrations at four sites from the CARE-China network, which were not assimilated. At the Beijing station, the NODA predictions are only half of the

DOI: 10.1021/acs.est.6b03745
Environ. Sci. Technol. 2017, 51, 2178–2185

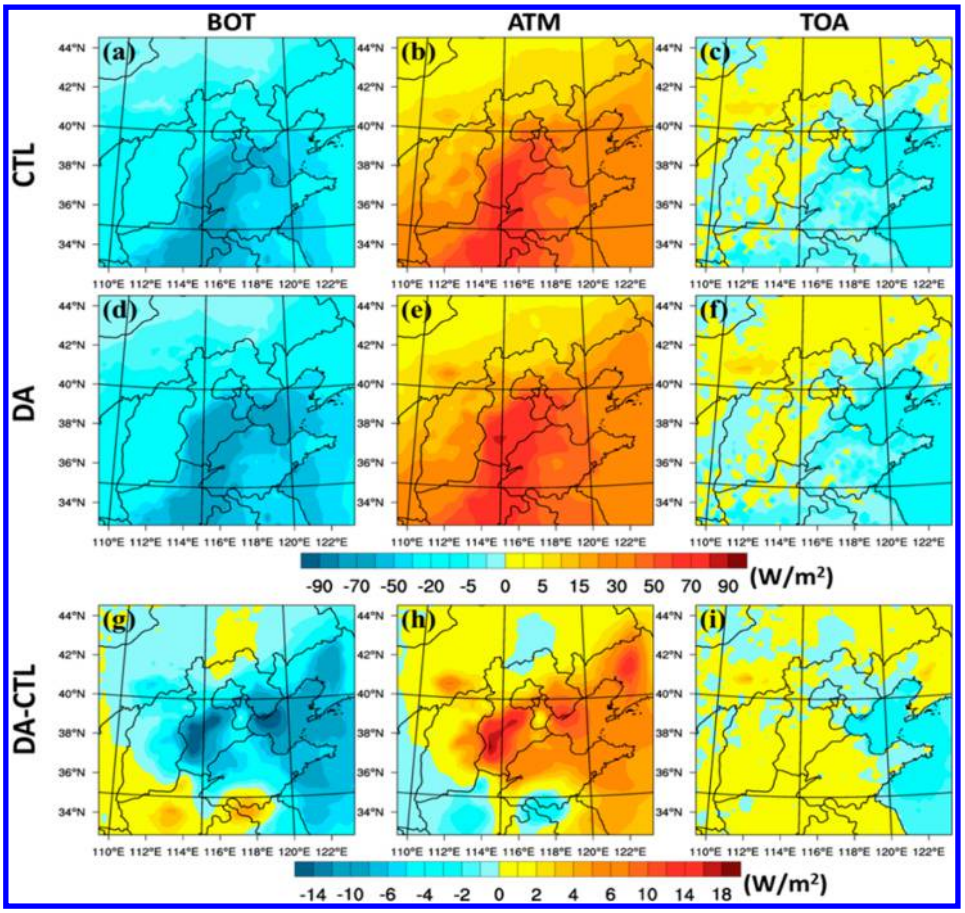

Figure 5. Monthly daytime all-sky ARF at the surface (BOT, positive values represent downward direction), inside the atmosphere (ATM, positive values indicate heating of the atmosphere) and at the top of the atmosphere (TOA, positive values denote downward direction) for CTL and DA cases; the last row refers to the differences between the CTL and DA cases.

peak hourly $PM_{2.5}$ and PM_{10} on January 13 (Figure 3(a, e)). The observed explosive increase is reproduced in the DA case, suggesting some severe pollution events can be captured by constraining initial conditions. The *R* value for $PM_{2.5}$ (PM_{10}) improved from 0.73 (0.71) to 0.86 (0.85), and RMSE is reduced from 95.9 $\mu g/m^3$ (136.3 $\mu g/m^3$) to 73.2 $\mu g/m^3$ (102.2 $\mu g/m^3$) (Table 2). Similar improvements in *R* and RMSE are found at the Tianjin and Xianghe stations (Table 2). At the Shijiazhuang station, the NODA forecasts show an opposite trend with observations. For example, predicted $PM_{2.5}$ and PM_{10} concentrations decrease from January 9 to 12, while observed $PM_{2.5}$ and PM_{10} concentrations show an increasing pattern. After DA, the correlation coefficient for $PM_{2.5}$ (PM_{10}) increases from −0.05 (0.00) to 0.68 (0.67) (Table 2). The improvements are also shown in reduced RMSE values (Table 2). The improvements in the Xianghe station are not as significant as in the other three stations (Table 2). This is mainly because Xianghe is located at the boundary between positive and negative increments. For example, at 01/21 00UTC, $PM_{2.5}$ concentration at Xianghe is supposed to increase (in positive increment area, Figure S4 in SI), but surrounding negative increments offset the impact and thus $PM_{2.5}$ concentrations do not increase much, as shown in Figure 3(d).The improvements in $PM_{2.5}$ predictions after assimilation also lead to changes in AOD. The spatial map of AOD differences (w and w/o DA) is similar to the spatial map of surface $PM_{2.5}$ differences, except in northwest Shandong areas (Figure 1(d, g)). The effects of assimilating surface $PM_{2.5}$ lead to 3-dimensional changes in $PM_{2.5}$, and these changes lead to changes in wind speed, direction and relative humidity and clouds due to the feedbacks. Thus, AOD changes may differ from surface $PM_{2.5}$ changes. Although only surface $PM_{2.5}$ is assimilated, the changes in surface aerosols can induce changes at higher altitudes due to vertical mixing and transport. As shown in the cross section plots in Figure 4, differences of monthly mean $PM_{2.5}$ concentrations (DA-NODA) reach over 80 $\mu g/m^3$ near the surface around latitude 41°N. The magnitudes of differences decrease with height, but are significant below 1km due to active boundary layer dynamics (Figure 4(d)).

We also evaluated AOD predictions using measurements from CSHNET, AERONET, MODIS, and CALIPSO. We used Angstrom exponent relations to derive model AOD at measurement wavelengths. The improvements in AOD at CSHNET and AERONET sites after DA are shown in Figure S5 and Table S1 in SI. After DA, MBE has been reduced from 0.67 to 0.64 at the Beijing station, and from 0.62 to 0.54 at the CAMS station The comparisons with MODIS and CALIPSO reflect that the spatial and vertical distributions of pollution are generally captured by the model, and DA has improved AOD and aerosol extinction predictions (SI Figure S6, S7, S8).

Impacts on Estimates of Health Impacts. Reducing the uncertainties in surface $PM_{2.5}$ concentrations provide better estimates of surface exposure and will reduce uncertainties in the estimated health impacts. Health impacts assessments were calculated following the method in Gao et al. (2015).[6] The assessed region is Jing-Jin-Ji area, as marked with blue box in Figure S1 in SI. Total mortality in January was estimated to be

DOI: 10.1021/acs.est.6b03745
Environ. Sci. Technol. 2017, 51, 2178−2185

Table 2. Statistics for Simulated $PM_{2.5}$ With and Without DA Compared against Non-Assimilated CARE-China Observations

	Beijing		Tianjin		Shijiazhuang		Xianghe	
	NODA	DA	NODA	DA	NODA	DA	NODA	DA
				$PM_{2.5}$				
R	0.73	0.86	0.67	0.75	−0.05	0.68	0.58	0.68
RMSE	95.9	73.2	173.6	96.9	190.9	136.1	50.2	61.4
				PM_{10}				
R	0.71	0.85	0.65	0.72	0.00	0.67	0.61	0.73
RMSE	136.3	102.2	164.8	104.6	261.8	160.7	144.3	127.3

7410 using unconstrained model surface $PM_{2.5}$ concentrations. After DA, this number increases to 7550. Using unconstrained model surface $PM_{2.5}$ concentrations (NODA), we estimated that 110.8 million (89.6% of Jing-Jin-Ji population) people are exposed to harmful air (defined with monthly averaged $PM_{2.5}$ concentration over 75 $\mu g/m^3$). After DA, this number changes to 113.9 million (92.1%).

Impacts on Estimates of Anthropogenic Radiative Forcing. We also calculated the impacts of integrating surface PM on estimates of anthropogenic radiative forcing (ARF). The anthropogenic ARF (including direct, semidirect, and indirect radiative forcing, monthly averaged daytime (8:00 to 17:00)) for the unconstrained case (i.e., radiation fluxes differences: NODA-ANT0), the constrained case (i.e., DA-ANT0) and their differences are shown in Figure 5. The spatial distribution of RF is similar to the results shown in Gao et al. (2014).[54] However, their values may be overestimated in west Shandong and east Henan and underestimated in Beijing and Hebei areas since the model overestimated AOD in Henan province and underestimated in Beijing and Hebei areas compared to MODIS and MISR.[54] Our constraints reduce AOD in Henan and increase AOD in Beijing and Hebei areas, suggesting improvements from previous study. Without DA, the domain mean forcing at the surface is −26.9 W/m^2, inside atmosphere is +24.2 W/m^2., and at the top of atmosphere is −2.7W/m^2. After DA, these numbers change by −3.0 (11.2%), 2.8 (11.6%), and −0.2W/m^2 (7.4%), respectively. These changes also result in changes in mixing heights (Figure S9 in SI), which further affects near surface $PM_{2.5}$ concentrations. The domain averaged monthly mean mixing heights decrease by 34 m due to DA.

These results demonstrate that observations from current networks of PM observations can be assimilated into contemporary coupled meteorology and chemistry models to produce $PM_{2.5}$ surface distributions with better quality. These distributions can lead to improved estimates in health impacts and anthropogenic ARF. Assimilation of near real-time surface $PM_{2.5}$ is also expected to lead to improvements in $PM_{2.5}$ forecasts (over 12 to 24 h). The fact that there are substantial changes in the distributions after assimilation reflects the fact that there are uncertainties in the model (due to estimates of emissions, incomplete knowledge of chemical processes, etc.). Further improvements in constraining $PM_{2.5}$ predictions will come from improvements in the forward model and its inputs.

■ ASSOCIATED CONTENT

Supporting Information

The Supporting Information is available free of charge on the ACS Publications website at DOI: 10.1021/acs.est.6b03745.

Model domain, emission map, $PM_{2.5}$ increments due to data assimilation, and verifications of AOD predictions (PDF)

■ AUTHOR INFORMATION

Corresponding Authors

*(M.G.) E-mail: meng-gao@uiowa.edu.

*(G.R.C.) Phone: 319-335-3332; fax: 319-335-3337; e-mail: gcarmich@engineering.uiowa.edu.

ORCID

Meng Gao: 0000-0002-8657-3541

Notes

The authors declare no competing financial interest.

■ ACKNOWLEDGMENTS

This work was supported in part by Grants from NASA Applied Science (NNX11AI52G) and EPA STAR (RD-83503701) programs. Special thanks are given to Yuesi Wang and his research group for providing measurements to evaluate model performance. Additionally, we thank Hong-Bin Chen, Philippe Goloub, Huizheng Che, Pucai Wang, and Xiangao Xia for their efforts in establishing and maintaining the AERONET sites used in this study.

■ REFERENCES

(1) van Donkelaar, A.; Martin, R. V.; Brauer, M.; Kahn, R.; Levy, R.; Verduzco, C.; Villeneuve, P. J. Global Estimates of Ambient Fine Particulate Matter Concentrations from Satellite-Based Aerosol Optical Depth: Development and Application. *Environ. Health Perspect.* **2010**, *118* (6), 847−855.

(2) Lim, S. S.; Vos, T.; Flaxman, A. D.; Danaei, G.; Shibuya, K.; Adair-Rohani, H.; Amann, M.; Anderson, H. R.; Andrews, K. G.; Aryee, M.; Atkinson, C.; Bacchus, L. J.; Bahalim, A. N.; Balakrishnan, K.; Balmes, J.; Barker-Collo, S.; Baxter, A.; Bell, M. L.; Blore, J. D.; Blyth, F.; Bonner, C.; Borges, G.; Bourne, R.; Boussinesq, M.; Brauer, M.; Brooks, P.; Bruce, N. G.; Brunekreef, B.; Bryan-Hancock, C.; Bucello, C.; Buchbinder, R.; Bull, F.; Burnett, R. T.; Byers, T. E.; Calabria, B.; Carapetis, J.; Carnahan, E.; Chafe, Z.; Charlson, F.; Chen, H.; Chen, J. S.; Cheng, A. T.-A.; Child, J. C.; Cohen, A.; Colson, K. E.; Cowie, B. C.; Darby, S.; Darling, S.; Davis, A.; Degenhardt, L.; Dentener, F.; Des Jarlais, D. C.; Devries, K.; Dherani, M.; Ding, E. L.; Dorsey, E. R.; Driscoll, T.; Edmond, K.; Ali, S. E.; Engell, R. E.; Erwin, P. J.; Fahimi, S.; Falder, G.; Farzadfar, F.; Ferrari, A.; Finucane, M. M.; Flaxman, S.; Fowkes, F. G. R.; Freedman, G.; Freeman, M. K.; Gakidou, E.; Ghosh, S.; Giovannucci, E.; Gmel, G.; Graham, K.; Grainger, R.; Grant, B.; Gunnell, D.; Gutierrez, H. R.; Hall, W.; Hoek, H. W.; Hogan, A.; Hosgood, H. D.; Hoy, D.; Hu, H.; Hubbell, B. J.; Hutchings, S. J.; Ibeanusi, S. E.; Jacklyn, G. L.; Jasrasaria, R.; Jonas, J. B.; Kan, H.; Kanis, J. a; Kassebaum, N.; Kawakami, N.; Khang, Y.-H.; Khatibzadeh, S.; Khoo, J.-P.; Kok, C.; Laden, F.; Lalloo, R.; Lan, Q.; Lathlean, T.; Leasher, J. L.; Leigh, J.; Li, Y.; Lin, J. K.; Lipshultz, S. E.; London, S.; Lozano, R.; Lu, Y.; Mak, J.; Malekzadeh, R.; Mallinger, L.; Marcenes, W.; March, L.; Marks, R.; Martin, R.; McGale, P.; McGrath, J.; Mehta, S.; Mensah, G. a; Merriman, T. R.; Micha, R.; Michaud, C.; Mishra, V.; Mohd Hanafiah, K.; Mokdad, A. a; Morawska, L.; Mozaffarian, D.; Murphy, T.; Naghavi, M.; Neal, B.; Nelson, P. K.; Nolla, J. M.; Norman, R.; Olives, C.; Omer, S. B.; Orchard, J.; Osborne, R.; Ostro, B.; Page, A.; Pandey, K. D.; Parry, C. D. H.;

DOI: 10.1021/acs.est.6b03745
Environ. Sci. Technol. 2017, 51, 2178−2185

Passmore, E.; Patra, J.; Pearce, N.; Pelizzari, P. M.; Petzold, M.; Phillips, M. R.; Pope, D.; Pope, C. A.; Powles, J.; Rao, M.; Razavi, H.; Rehfuess, E. a; Rehm, J. T.; Ritz, B.; Rivara, F. P.; Roberts, T.; Robinson, C.; Rodriguez-Portales, J. a; Romieu, I.; Room, R.; Rosenfeld, L. C.; Roy, A.; Rushton, L.; Salomon, J. a; Sampson, U.; Sanchez-Riera, L.; Sanman, E.; Sapkota, A.; Seedat, S.; Shi, P.; Shield, K.; Shivakoti, R.; Singh, G. M.; Sleet, D. a; Smith, E.; Smith, K. R.; Stapelberg, N. J. C.; Steenland, K.; Stöckl, H.; Stovner, L. J.; Straif, K.; Straney, L.; Thurston, G. D.; Tran, J. H.; Van Dingenen, R.; van Donkelaar, A.; Veerman, J. L.; Vijayakumar, L.; Weintraub, R.; Weissman, M. M.; White, R. a; Whiteford, H.; Wiersma, S. T.; Wilkinson, J. D.; Williams, H. C.; Williams, W.; Wilson, N.; Woolf, A. D.; Yip, P.; Zielinski, J. M.; Lopez, A. D.; Murray, C. J. L.; Ezzati, M.; AlMazroa, M. a; Memish, Z. a A Comparative Risk Assessment of Burden of Disease and Injury Attributable to 67 Risk Factors and Risk Factor Clusters in 21 Regions, 1990−2010: A Systematic Analysis for the Global Burden of Disease Study 2010. *Lancet* **2012**, *380* (9859), 2224−2260.

(3) Gao, M.; Carmichael, G. R.; Wang, Y.; Saide, P. E.; Yu, M.; Xin, J.; Liu, Z.; Wang, Z. Modeling Study of the 2010 Regional Haze Event in the North China Plain. *Atmos. Chem. Phys.* **2016**, *16* (3), 1673−1691.

(4) Gao, M.; Carmichael, G. R.; Saide, P. E.; Lu, Z.; Yu, M.; Streets, D. G.; Wang, Z. Response of Winter Fine Particulate Matter Concentrations to Emission and Meteorology Changes in North China. *Atmos. Chem. Phys.* **2016**, *16*, 11837−11851.

(5) Gao, M.; Carmichael, G. R.; Wang, Y.; Ji, D.; Liu, Z.; Wang, Z. Improving Simulations of Sulfate Aerosols during Winter Haze over Northern China: The Impacts of Heterogeneous Oxidation by NO_2. *Front. Environ. Sci. Eng.*. 2016, *10* (5), p16.

(6) Gao, M.; Guttikunda, S. K.; Carmichael, G. R.; Wang, Y.; Liu, Z.; Stanier, C. O.; Saide, P. E.; Yu, M. Health Impacts and Economic Losses Assessment of the 2013 Severe Haze Event in Beijing Area. *Sci. Total Environ.* **2015**, *511* (January 2013), 553−561.

(7) Seinfeld, J. H.; Pandis, S. N. *Atmospheric Chemistry and Physics: from Air Pollution to Climate Change*, 3rd ed.; John Wiley & Sons: Hoboken, NJ, 2016.

(8) Kumar, R.; Barth, M. C.; Pfister, G. G.; Naja, M.; Brasseur, G. P. WRF-Chem Simulations of a Typical Pre-Monsoon Dust Storm in Northern India: Influences on Aerosol Optical Properties and Radiation Budget. *Atmos. Chem. Phys.* **2014**, *14* (5), 2431−2446.

(9) Carmichael, G. R.; Sandu, A.; Chai, T.; Daescu, D. N.; Constantinescu, E. M.; Tang, Y. Predicting Air Quality: Improvements through Advanced Methods to Integrate Models and Measurements. *J. Comput. Phys.* **2008**, *227* (7), 3540−3571.

(10) Niu, T.; Gong, S. L.; Zhu, G. F.; Liu, H. L.; Hu, X. Q.; Zhou, C. H.; Wang, Y. Q. Data Assimilation of Dust Aerosol Observations for CUACE/Dust Forecasting System. *Atmos. Chem. Phys. Discuss.* **2007**, *7*, 8309−8332.

(11) Schwartz, C. S.; Liu, Z.; Lin, H.-C.; McKeen, S. a. Simultaneous Three-Dimensional Variational Assimilation of Surface Fine Particulate Matter and MODIS Aerosol Optical Depth. *J. Geophys. Res.* **2012**, *117* (D13), D13202.

(12) Pagowski, M.; Grell, G. a. Experiments with the Assimilation of Fine Aerosols Using an Ensemble Kalman Filter. *J. Geophys. Res. Atmos.* **2012**, *117* (November), 1−15.

(13) Tombette, M.; Mallet, V.; Sportisse, B. PM_{10} Data Assimilation over Europe with the Optimal Interpolation Method. *Atmos. Chem. Phys.* **2009**, *9*, 57−70.

(14) Elbern, H.; Schmidt, H.; Ebel, A. For Tropospheric Chemistry Modeling Linear Version of the Model. The Procedure Is Commonly. *J. Geophys. Res.* **1997**, *102* (97).

(15) Elbern, H.; Schmidt, H.; Talagrand, O.; Ebel, a. 4D-Variational Data Assimilation with an Adjoint Air Quality Model for Emission Analysis. *Environ. Model. Softw.* **2000**, *15*, 539−548.

(16) Elbern, H.; Schmid, H. A Four-Dimensional Variational Chemistry Data Assimilation Scheme for Eulerian Chemistry Transport Modeling. *J. Geophys. Res.* **1999**, *104* (D5), 18583−18598.

(17) Elbern, H.; Schmidt, H. Ozone Episode Analysis by Four-Dimensional Variational Chemistry Data Assimilation. *J. Geophys. Res.* **2001**, *106*, 3569.

(18) Chai, T.; Carmichael, G. R.; Sandu, A.; Tang, Y.; Daescu, D. N. Chemical Data Assimilation of Transport and Chemical Evolution over the Pacific (TRACE-P) Aircraft Measurements. *J. Geophys. Res.* **2006**, *111* (Cmc), 1−18.

(19) Chai, T.; Carmichael, G. R.; Tang, Y.; Sandu, A.; Hardesty, M.; Pilewskie, P.; Whitlow, S.; Browell, E. V.; Avery, M. a.; Nédélec, P.; Merrill, J. T.; Thompson, A. M.; Williams, E. Four-Dimensional Data Assimilation Experiments with International Consortium for Atmospheric Research on Transport and Transformation Ozone Measurements. *J. Geophys. Res.* **2007**, *112*, 1−18.

(20) Adhikary, B.; Kulkarni, S.; Dallura, a.; Tang, Y.; Chai, T.; Leung, L. R.; Qian, Y.; Chung, C. E.; Ramanathan, V.; Carmichael, G. R. A Regional Scale Chemical Transport Modeling of Asian Aerosols with Data Assimilation of AOD Observations Using Optimal Interpolation Technique. *Atmos. Environ.* **2008**, *42* (37), 8600−8615.

(21) Collins, W. D.; Rasch, P. J.; Eaton, B. E.; Khattatov, B. V.; Lamarque, J. F.; Zender, C. S. Simulating aerosols using a chemical transport model with assimilation of satellite aerosol retrievals: Methodology for INDOEX. *J. Geophys. Res. Atmos.* **2016**, *106* (D7), 7313−7336.

(22) Zhang, J.; Reid, J. S.; Westphal, D. L.; Baker, N. L.; Hyer, E. J. A system for operational aerosol optical depth data assimilation over global oceans. *J. Geophys. Res.* **2008**, *113* (D10), D10208.

(23) Chen, D.; Liu, Z.; Schwartz, C. S.; Lin, H.-C.; Cetola, J. D.; Gu, Y.; Xue, L. The Impact of Aerosol Optical Depth Assimilation on Aerosol Forecasts and Radiative Effects during a Wild Fire Event over the United States. *Geosci. Model Dev.* **2014**, *7*, 2709−2715.

(24) Jiang, Z.; Liu, Z.; Wang, T.; Schwartz, C. S.; Lin, H. C.; Jiang, F. Probing into the Impact of 3DVAR Assimilation of Surface PM10 Observations over China Using Process Analysis. *J. Geophys. Res. Atmos.* **2013**, *118*, 6738−6749.

(25) Liu, Z.; Liu, Q.; Lin, H.-C.; Schwartz, C. S.; Lee, Y.-H.; Wang, T. Three-Dimensional Variational Assimilation of MODIS Aerosol Optical Depth: Implementation and Application to a Dust Storm over East Asia. *J. Geophys. Res. Atmos.* **2011**, *116* (D23), n/a−n/a.n/a10.1029/2011JD016159

(26) Pagowski, M.; Grell, G. a.; McKeen, S. a.; Peckham, S. E.; Devenyi, D. Three-Dimensional Variational Data Assimilation of Ozone and Fine Particulate Matter Observations: Some Results Using the Weather Research and Forecasting-Chemistry Model and Grid-Point Statistical Interpolation. *Q. J. R. Meteorol. Soc.* **2010**, *136* (October 2010), 2013−2024.

(27) Saide, P. E.; Carmichael, G. R.; Liu, Z.; Schwartz, C. S.; Lin, H. C.; da Silva, a. M.; Hyer, E. Aerosol Optical Depth Assimilation for a Size-Resolved Sectional Model: Impacts of Observationally Constrained, Multi-Wavelength and Fine Mode Retrievals on Regional Scale Analyses and Forecasts. *Atmos. Chem. Phys.* **2013**, *13* (20), 10425−10444.

(28) Saide, P. E.; Kim, J.; Song, C. H.; Choi, M.; Cheng, Y.; Carmichael, G. R. Assimilation of next generation geostationary aerosol optical depth retrievals to improve air quality simulations. *Geophysical research letters.* **2014**, *41*, 2014GL062089.

(29) Saide, P. E.; Spak, S. N.; Pierce, R. B.; Otkin, J. A.; Schaack, T. K.; Heidinger, A. K.; da Silva, A. M.; Kacenelenbogen, M.; Redemann, J.; Carmichael, G. R. Central American biomass burning smoke can increase tornado severity in the U.S. *Geophysical research letters* **2015**, *42*, 2014GL062826.

(30) Benedetti, A.; Morcrette, J. J.; Boucher, O.; Dethof, A.; Engelen, R. J.; Fisher, M.; Flentje, H.; Huneeus, N.; Jones, L.; Kaiser, J. W.; Kinne, S. Aerosol analysis and forecast in the European centre for medium-range weather forecasts integrated forecast system: 2. Data assimilation. *J. Geophys. Res.* **2009**, *114*(D13).10.1029/2008JD011115

(31) Rubin, J. I.; Collins, W. D. Global simulations of aerosol amount and size using MODIS observations assimilated with an Ensemble Kalman Filter. *J. Geophys. Res. Atmos.* **2014**, *119*(22).12,78010.1002/2014JD021627

DOI: 10.1021/acs.est.6b03745
Environ. Sci. Technol. 2017, 51, 2178−2185

(32) Rubin, J. I.; Reid, J. S.; Hansen, J. A.; Anderson, J. L.; Collins, N.; Hoar, T. J.; Hogan, T.; Lynch, P.; McLay, J.; Reynolds, C. A.; Sessions, W. R. Development of the Ensemble Navy Aerosol Analysis Prediction System (ENAAPS) and its application of the Data Assimilation Research Testbed (DART) in support of aerosol forecasting. *Atmos. Chem. Phys. Discuss.* **2016**, *15*(20).2806910.5194/acpd-15-28069-2015

(33) Lin, C.; Wang, Z.; Zhu, J. An Ensemble Kalman Filter for Severe Dust Storm Data Assimilation over China. *Atmos. Chem. Phys.* **2008**, *8* (2007), 2975−2983.

(34) Schutgens, N. a. J.; Miyoshi, T.; Takemura, T.; Nakajima, T. Applying an Ensemble Kalman Filter to the Assimilation of AERONET Observations in a Global Aerosol Transport Model. *Atmos. Chem. Phys. Discuss.* **2009**, *9*, 23835−23873.

(35) Sessions, W. R.; Reid, J. S.; Benedetti, A.; Colarco, P. R.; da Silva, A.; Lu, S.; Sekiyama, T.; Tanaka, T. Y.; Baldasano, J. M.; Basart, S.; Brooks, M. E. Development towards a global operational aerosol consensus: basic climatological characteristics of the International Cooperative for Aerosol Prediction Multi-Model Ensemble (ICAP-MME). *Atmos. Chem. Phys.* **2015**, *15*, 335−362.

(36) Bocquet, M.; Elbern, H.; Eskes, H.; Hirtl, M.; Žabkar, R.; Carmichael, G. R.; Flemming, J.; Inness, a.; Pagowski, M.; Pérez Camaño, J. L.; Saide, P. E.; San Jose, R.; Sofiev, M.; Vira, J.; Baklanov, a.; Carnevale, C.; Grell, G.; Seigneur, C. Data Assimilation in Atmospheric Chemistry Models: Current Status and Future Prospects for Coupled Chemistry Meteorology Models. *Atmos. Chem. Phys.* **2015**, *15* (10), 5325−5358.

(37) Emmons, L. K.; Walters, S.; Hess, P. G.; Lamarque, J.-F.; Pfister, G. G.; Fillmore, D.; Granier, C.; Guenther, a.; Kinnison, D.; Laepple, T.; Orlando, J.; Tie, X.; Tyndall, G.; Wiedinmyer, C.; Baughcum, S. L.; Kloster, S. Description and Evaluation of the Model for Ozone and Related Chemical Tracers, Version 4 (MOZART-4). *Geosci. Model Dev.* **2010**, *3* (1), 43−67.

(38) Zaveri, R. a.; Peters, L. K. A New Lumped Structure Photochemical Mechanism for Large-Scale Applications. *J. Geophys. Res. Atmos* **1999**, *104* (D23), 30387−30415.

(39) Zaveri, R. a.; Easter, R. C.; Fast, J. D.; Peters, L. K. Model for Simulating Aerosol Interactions and Chemistry (MOSAIC). *J. Geophys. Res.* **2008**, *113* (D13), D13204.

(40) Iacono, M. J.; Delamere, J. S.; Mlawer, E. J.; Shephard, M. W.; Clough, S. a.; Collins, W. D. Radiative Forcing by Long-Lived Greenhouse Gases: Calculations with the AER Radiative Transfer Models. *J. Geophys. Res.* **2008**, *113* (D13), D13103.

(41) Hong, Song-You; Noh, Yign; Dudhia, J. A New Vertical Diffusion Package with an Explicit Treatment of. *Mon. Weather Rev.* **2006**, *134* (9), 2318−2341.

(42) Lin, Yuh-Lang; Farley, Richard D.; Orville, H. D. Bulk Parameterization of the Snow Field in a Cloud Model. *J. Clim. Appl. Meteorol.* **1983**, *22* (6), 1065−1092.

(43) Grell, G. A. Prognostic Evaluation of Assumptions Used by Cumulus Parameterizations. *Mon. Weather Rev.* **1993**, *121*, 764−787.

(44) Li, M.; Zhang, Q.; Kurokawa, J.; Woo, J.-H.; He, K. B.; Lu, Z.; Ohara, T.; Song, Y.; Streets, D. G.; Carmichael, G. R.; Cheng, Y. F.; Hong, C. P.; Huo, H.; Jiang, X. J.; Kang, S. C.; Liu, F.; Su, H.; Zheng, B. MIX: A Mosaic Asian Anthropogenic Emission Inventory for the MICS-Asia and the HTAP Projects. *Atmos. Chem. Phys. Discuss.* **2015**, *15*, 34813−34869.

(45) Guenther, A.; Karl, T.; Harley, P.; Wiedinmyer, C.; Palmer, P. I.; Geron, C. Estimates of Global Terrestrial Isoprene Emissions Using MEGAN (Model of Emissions of Gases and Aerosols from Nature). *Atmos. Chem. Phys. Discuss.* **2006**, *6* (1), 107−173.

(46) Ginoux, P.; Chin, M.; Tegen, I.; Goddard, T. In-, G. Sources and Distributions of Dust Aerosols Simulated with the GOCART Model. *J. Geophys. Res.* **2001**, *106* (D17), 20255−20273.

(47) Parrish, David F.; Derber, J. C. The National Meteorological Center's Spectral Statistical-Interpolation Analysis System. *Mon. Weather Rev.* **1992**, *120*, 1747−1763.

(48) Elbern, H.; Strunk, a.; Schmidt, H.; Talagrand, O. Emission Rate and Chemical State Estimation by 4-Dimensional Variational Inversion. *Atmos. Chem. Phys.* **2007**, *7*, 3749−3769.

(49) Rizvi, S.; Liu, Z.; Huang, X. Generation of WRF-ARW background errors (BE) for GSI, NCAR/ESSL/MMM, http://www.dtcenter.org/com-GSI/users/docs/write_ups/WRF-ARW-GSI_BE.pdf (accessed January 2017).

(50) Xin, J.; Wang, Y.; Pan, Y.; Ji, D.; Liu, Z.; Wen, T.; Wang, Y.; Li, X.; Sun, Y.; Sun, J.; Wang, P.; Wang, G.; Wang, X.; Cong, Z.; Song, T.; Hu, B.; Wang, L.; Tang, G.; Gao, W.; Guo, Y.; Miao, H.; Tian, S.; Wang, L. The Campaign on Atmospheric Aerosol Research Network of China: CARE-China. *Bull. Am. Meteorol. Soc.* **2015**, *96* (7), 1137−1155.

(51) Xin, J.; Wang, Y.; Li, Z.; Wang, P.; Hao, W. M.; Nordgren, B. L.; Wang, S.; Liu, G.; Wang, L.; Wen, T.; Sun, Y.; Hu, B. Aerosol Optical Depth (AOD) and Ångström Exponent of Aerosols Observed by the Chinese Sun Hazemeter Network from August 2004 to September 2005. *J. Geophys. Res.* **2007**, *112* (D5), D05203.

(52) Holben, B. N.; Eck, T. F.; Slutsker, I.; Tanre, D.; Vermote, E.; Reagan, J. A.; Kaufman, Y. J.; Nakajima, T.; Lavenu, F.; Jankowiak, I.; Smirnov, A. AERONET — A Federated Instrument Network and Data Archive for Aerosol Characterization. *Remote Sens. Environ.* **1998**, *66* (1), 1−16.

(53) Cheng, Y.; Zheng, G.; Wei, C.; Mu, Q.; Zheng, B.; Wang, Z.; Gao, M.; Zhang, Q.; He, K.; Carmichael, G.; Pöschl, U. Reactive nitrogen chemistry in aerosol water as a source of sulfate during haze events in China. *Science Advances* **2016**, *2* (12), e1601530.

(54) Gao, Y.; Zhao, C.; Liu, X.; Zhang, M.; Leung, L. R. WRF-Chem Simulations of Aerosols and Anthropogenic Aerosol Radiative Forcing in East Asia. *Atmos. Environ.* **2014**, *92*, 250−266.

DOI: 10.1021/acs.est.6b03745
Environ. Sci. Technol. 2017, 51, 2178−2185